Spontaneous Onion-Structure Formation from Planar Lamellar Nuclei

Yasutaka Iwashita and Hajime Tanaka*

Institute of Industrial Science, University of Tokyo, Meguro-ku, Tokyo 153-8505, Japan

(Received 28 September 2006; published 6 April 2007)

Nucleation and growth are a basic elementary process of ordering. The nucleation process is controlled by a competition between interfacial and bulk energy. Thus an ordered structure of a nucleus at its birth is not necessarily the most stable thermodynamically: Ostwald step rule. In addition to this, we found the topological transformation of nuclei from the most stable bulk structure (planar lamella) to a metastable one (onion) in a lyotropic liquid crystal. This indicates that the fate of nuclei of low-dimensional internal order can also be seriously affected by an additional competition between interfacial and elastic deformation energy.

DOI: 10.1103/PhysRevLett.98.145703 PACS numbers: 64.60.Qb, 64.60.My, 64.70.Md, 81.16.Dn

Physical factors controlling the kinetic pathway of homogeneous nucleation of an ordered phase from a disordered one have been a key question in materials science since Ostwald formulated his step rule over a century ago [1]. According to the classical nucleation theory, the size of a critical nucleus is $R_c = 2\sigma/\Delta\mu$, where σ is the interfacial tension and $\Delta\mu$ is the chemical potential difference between the ordered and disordered phase, and the height of the nucleation barrier is $\Delta G^* = 16\pi\sigma^3/3\Delta\mu^2$. Thus, ΔG^* is lower for smaller σ and larger $\Delta\mu$. However, these two requirements generally compete with each other. For a simple liquid, the following pathway was demonstrated (e.g., [2]): The structure of the precritical nuclei is that of a metastable body-center cubic crystal (bcc). As the nuclei grow, the structure in the core transforms into that of the stable face-center cubic crystal (fcc), while retaining the metastable structure in the interface region. This is basically consistent with the Ostwald step rule. This is a consequence of the lower nucleation barrier for the bcc structure: Although bcc has a higher free energy than fcc, the interfacial energy is lower for the former than the latter. Similar behavior was also observed experimentally for the ordering in proteins [3]. In these examples, a metastable structure is transiently selected to lower the nucleation barrier via the reduction of interfacial energy. However, the final structure should be the stable equilibrium one since the relative contribution of the interfacial energy decreases as nuclei grow. Here we report that this final statement is not necessarily true for ordering into a low-dimensional order, taking smectic ordering of a lyotropic liquid crystal as an example.

We used a lyotropic liquid crystal [4]: a mixture of water and nonionic surfactant, $C_{10}E_3$ (triethyleneglycol mono *n*-decyl ether) (see [5] for the phase diagram). In water the surfactant molecules spontaneously form bilayer membranes, which further form a higher order membrane organization (e.g., sponge and lamella). This system is characterized by the extremely large intermembrane spacing d (e.g., about 0.1 μm for the concentration $\phi =$ 3 wt. %; $\sim 10^3$ times larger than atomic systems). This large length scale enables us to ''directly'' observe the initial process of nucleation and growth (NG) of the lamellar phase with optical microscopy. The large characteristic timescale ($\propto d^3$; $\sim 10^9$ times slower than atomic systems) [6,7] also allows us to follow the process in real time. In this study we cooled a sample from the one-phase sponge region to the lamellar-sponge coexisting region to observe homogeneous nucleation of the lamellar phase with an optical microscope (Olympus BX51).

For $\phi =$ 2–10 wt. %, the nucleation rate is rather low for a shallow quench. Thus, we can observe the NG process of an individual nucleus without interference from other nuclei (no overlap of depletion zones). After quench, the lamellar phase is homogeneously nucleated. By observing the nuclei from various orientations (Fig. 1), we confirmed that the lamellar nuclei actually have a lens shape. Interestingly, as they grow they change their shape from lens to sphere (Fig. 1). This shape transformation proceeds while keeping axisymmetry (cylindrical symmetry): Upon transformation, the edge of a lens-shaped nucleus remains circular and the curved nucleus has ''cuplike'' geometry (see the arrowed nuclei in Fig. 1, whose axisymmetric axes lie almost on the image plane).

A typical lens-to-sphere shape transformation process observed from its side is shown in Figs. 2(a) and 2(b). When a lens-shaped nucleus grows to a certain size [$\sim$20 μm, slightly after the time of the leftmost image in

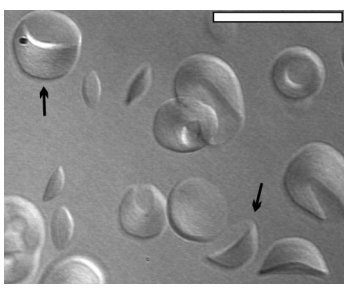

FIG. 1. Spontaneous shape transformation from lens to onion structure ($\phi =$ 2.0 wt. %; 30.9 °C). Scale bar = 100 μm.

 © 2007 The American Physical Society

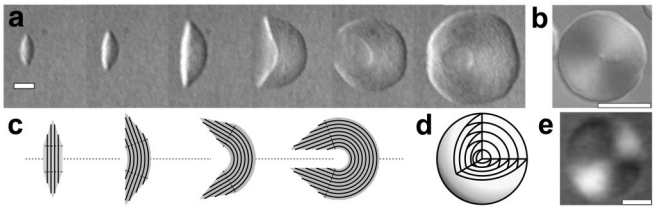

FIG. 2. (a) A growing lamellar nucleus ($\phi = 2.0$ wt. %; 31.2 °C). The elapsed time from its nucleation is 4.0, 12.0, 36.0, 60.0, 84.0, and 144.0 s, respectively, from the left. (b) An onion nucleus observed at a few minutes after the shape transformation ($\phi = 4.9$ wt. %; 34.4 °C). (a) and (b) were observed with differential interference microscopy. (c) Schematic representation for the change of membrane organization during the shape transformation. The dotted line indicates their symmetric axis. (d) Structure of an onion nucleus. (e) An onion nucleus observed with polarizing microscopy with a compensator ($\phi =$ 3.1 wt. %; 32.1 °C). The optical axes of the polarizer and analyzer are aligned approximately 45° to the sides of the images for (a), whereas they are parallel to the horizontal and vertical sides for (b) and (e). Scale bars correspond to 10 μm for (a) and (e), while 50 μm for (b).

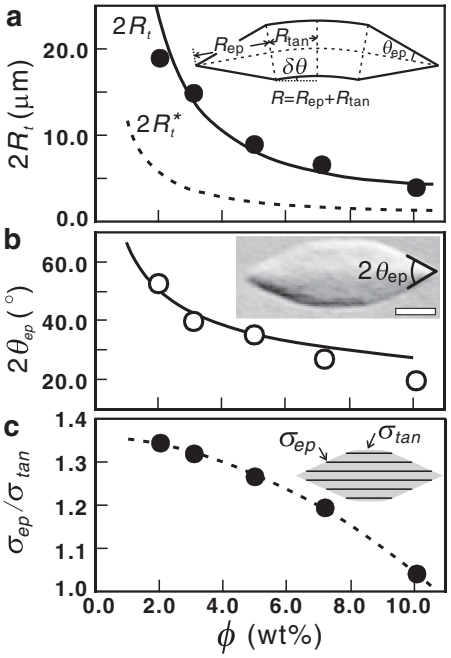

FIG. 3. (a) ϕ dependence of $2R_t$. The solid curve is calculated by the linear stability analysis. The dotted curve represents $2R_t^*$ (see text). The inset shows the deformation mode (represented by $\delta\theta$), which leads to the shape transformation. (b) ϕ dependence of $2\theta_{ep}$. The solid curve is the theoretical prediction. The inset is a lens-shaped nucleus observed with differential interference microscopy from its side ($\phi = 2.0$ wt. %; 30.9 °C). (c) ϕ dependence of σ_{ep}/σ_{tan} with the fitted curve.

Fig. 2(a)], it starts bending (the second image from the left). The remaining sponge phase around the center of the rightmost nucleus in Fig. 2(a) gradually transforms into the lamellar phase and thus a nucleus eventually forms a completely spherical domain, or onion structure [Fig. 2(b)]. Once a lens-shaped nucleus starts bending, it does not stop bending until a complete transformation into a spherical shape. This means that a lens shape is intrinsically unstable against a spherical one above the critical radius of a lens, R_t. We confirmed that this shape transformation process crucially depends on ϕ: R_t as well as the time to shape transformation decrease with an increase in ϕ. Figure 3(a) shows the ϕ dependence of $2R_t$. At high ϕ ($\phi \sim$ 20–40 wt. %), the quench depth necessary for inducing homogeneous nucleation is typically about 1.0 K [8], which is larger than that at low ϕ (about 0.1 K). This leads to large undercooling at these concentrations, which drastically accelerates the NG process. Around $\phi = 20$ wt. %, we confirmed that the shape transformation occurs within $\sim$0.1 s, using a high speed camera. Furthermore, we saw an unstable growth accompanying shape instability (probably Mullins-Sekerka type) for a deep quench.

Next we explain a membrane configuration inside the nuclei. From observation with polarizing microscopy, we confirmed that the principal optical axis of a lens-shaped nucleus is perpendicular to the plane of its circular edge: This further means that the nucleus consists of a planar lamellar structure, which is parallel to the plane of its circular edge, as shown in Fig. 2(c), since the principal optical axis of the membrane is perpendicular to it. This type of a lamellar nucleus is known to be formed (cf. Ref. [9]) when the epitaxial relation at the lamellar-sponge interface is satisfied [10,11], i.e., membranes are continuous through the interface. A geometrical condition for matching the intermembrane spacing of the lamellar phase d_α to that of the sponge phase d_3 is given by $\sin\theta_{ep} \simeq d_\alpha/d_3$ (for the definition of θ_{ep}, see Fig. 3). The measured values of θ_{ep} are consistent with the above theoretical prediction if we properly take fluctuation effects on the intermembrane spacing [4] into account [Fig. 3(b)]. This indicates that the epitaxial relation is really satisfied at the interface. From the shape of a nucleus, we also determined the ratio between the interfacial tension for the epitaxial interface σ_{ep} and that for the tangential interface σ_{tan}, using Wulff's theorem [9]. For simplicity, only the two orientations are considered here. The ϕ dependence of σ_{ep}/σ_{tan} is shown in Fig. 3(c).

We also observed a spherical nucleus by polarizing microscopy with a compensator [Fig. 2(e)]: The brighter and darker areas correspond to positive and negative optical retardation, respectively. This means that membranes are aligned parallel to the interface. Considering the transformation process from lens to onion structure [Fig. 2(c)], we conclude that the spherical nucleus has an onion structure, or a multilamellar vesicle structure [12] [Fig. 2(d)]. Here it may be worth noting that the core size should be larger than d and may be comparable to the penetration depth (see, e.g., [4]), which is ignored in the figure.

Now we consider the mechanism of the transformation from lens to onion structure. The total energy of a nucleus relevant to shape selection is given by the sum of the elastic energy E_{ela} and the interfacial energy E_{int}. For a lens-

shaped nucleus, $E_{\rm lens} = E_{\rm ela}^{\rm lens} + E_{\rm int}^{\rm lens}$: $E_{\rm ela}^{\rm lens} = 0$ and $E_{\rm int}^{\rm lens} \simeq S_{\rm lens}\sigma$ [13], where $S_{\rm lens}$ is the interfacial area of a lens-shaped nucleus. For an onion nucleus, on the other hand, $E_{\rm onion} = E_{\rm ela}^{\rm onion} + E_{\rm int}^{\rm onion}$: $E_{\rm ela}^{\rm onion} \simeq 4\pi(2\kappa + \kappa_g)R_{\rm onion}/d_\alpha$ and $E_{\rm int}^{\rm onion} \simeq S_{\rm onion}\sigma$, where $R_{\rm onion}$ is the radius of an onion structure and κ and κ_g are the mean and Gaussian curvature elastic modulus of a membrane, respectively. Note that $\sigma \simeq \kappa/d_3^2$ [10,11,14]. We estimate the critical size R_t^* from $E_{\rm onion} - E_{\rm lens} = 4\pi(2\kappa + \kappa_g)R_t^*/d_\alpha - \Delta S(R_t^*)\sigma = 0$, imposing the constant volume condition. Here $\Delta S = S_{\rm lens} - S_{\rm onion} > 0$. Assuming $\Delta S(R) = c_s R^2$ (c_s is a constant) and $d_\alpha \sim d_3 \equiv d$, we obtain $R_t^* \sim [4\pi(2 + \kappa_g/\kappa)d]/c_s \sim 40d$. The final relation is based on the following order estimations: $c_s \simeq (S_{\rm lens} - S_{\rm onion})/R^2 \sim 1$ and $\kappa \sim \kappa_g \sim k_BT$. Note that $\phi \simeq \psi = \delta/d$, where ψ is the volume fraction of surfactant and δ ($\cong$2.8 nm) is the membrane thickness. Here $\psi = 1/\{1 + (\rho_s/\rho_w) \times (\phi^{-1} - 1)\} \simeq \phi$, where the density of water $\rho_w \simeq 0.995\ {\rm g\,cm^{-3}}$ and that of $C_{10}E_3$ $\rho_s = 0.938\ {\rm g\,cm^{-3}}$. Thus, $R_t^* \propto \phi^{-1}$, which explains the observed trend but does not explain the magnitude [Fig. 3(a)].

To determine the onset of instability, or the critical radius R_t, however, we need to make a linear stability analysis for an infinitesimal deformation of a lens-shaped nucleus. We take an axisymmetric deformation illustrated in the inset of Fig. 3(a) as the deformation mode, represented by $\delta\theta$. Then we determine $R_t = R_{\rm ep} + R_{\rm tan}$ from the condition $\delta E/\delta\theta = 0$. Note that we have a relation $R_{\rm tan}/R_{\rm ep} = \sigma_{\rm ep}/(\sigma_{\rm tan}\cos\theta_{\rm ep}) - 1$, where we can directly measure $R_{\rm tan}/R_{\rm ep}$ and $\theta_{\rm ep}$ [Figs. 3(b) and 3(c)]. For simplicity, we ignore the deformation of the edge part of a lens. First we consider the $\delta\theta$ dependence of $E_{\rm ela}$ due to the deformation of the central tangential part: $\delta E_{\rm ela}/\delta\theta \simeq \delta\{2\pi(2\kappa + \kappa_g)(2R_{\rm ep}\tan\theta_{\rm ep})/d_\alpha)[1 - \cos(2\delta\theta)]\}/\delta\theta \simeq 16\pi(2\kappa + \kappa_g)(R_{\rm ep}\tan\theta_{\rm ep}/d_\alpha)\delta\theta$. Next we estimate the $\delta\theta$ dependence of $E_{\rm int}$. Since the volume is imposed to be constant during the deformation, it is convenient to introduce a form factor g_s as the ratio of the surface area of a domain to that of the sphere having the same volume as its volume V: $g_s = (S/4\pi)/(3V/4\pi)^{2/3}$. For our case, $g_s \sim \beta - \alpha\delta\theta^2$, where α and β are positive constants, provided $\delta\theta \ll 1$. Thus, $\delta E_{\rm int}/\delta\theta = \sigma_{\rm ep}\delta S_{\rm ep}/\delta\theta + \sigma_{\rm tan}\delta S_{\rm tan}/\delta\theta \simeq -2[4\pi(3V/4\pi)^{2/3}] \times (\alpha_{\rm ep}\sigma_{\rm ep} + \alpha_{\rm tan}\sigma_{\rm tan})\delta\theta = -(c_g^{\rm ep}\sigma_{\rm ep} + c_g^{\rm tan}\sigma_{\rm tan})R_{\rm ep}^2\delta\theta$, where the subscripts ep and tan denote that the values are of the epitaxial and tangential part, respectively. We numerically estimated $c_g^{\rm ep}(\phi)$ and $c_g^{\rm tan}(\phi)$ with the measured values $\theta_{\rm ep}$ and $R_{\rm ep}/R_{\rm tan}$. The total energy controlling the shape transformation is thus given by $\delta E/\delta\theta = \delta E_{\rm ela}/\delta\theta + \delta E_{\rm int}/\delta\theta$. From $\delta E/\delta\theta = 0$ we can determine $R_{\rm ep}$ and thus $R_t = R_{\rm ep} + R_{\rm tan}$ from the above-mentioned relation between $R_{\rm ep}$ and $R_{\rm tan}$. R_t estimated in this way with $\kappa = k_BT$ and $\kappa_g = 0.7k_BT$ well reproduces the measured R_t [Fig. 3(a)], which support our mechanism. Here we note that $R_t^* < R_t$, indicating the existence of the energy barrier for the shape transformation for $R_t^* < R < R_t$ [Fig. 4(b)].

In the above, we ignore the decrease of $\bar\sigma_{\rm lens}$ during the shape transformation, for simplicity [13]. The ratio of the estimate considering the change in the total interfacial area alone (assuming no change in $\bar\sigma_{\rm lens}$) to that considering also the anisotropy of the interfacial tension is estimated as $\sim(\alpha_{\rm ep} + \alpha_{\rm tan})\bar\sigma_{\rm lens}/(\alpha_{\rm ep}\sigma_{\rm ep} + \alpha_{\rm tan}\sigma_{\rm tan})$. According to our numerical estimation, this ratio varies from 0.99 for $\phi =$ 10 wt. % to 0.8 for 2.0 wt. %. Thus, we may say that the decrease of the total interfacial area is the main cause of the reduction of the interfacial energy at least for $\phi \geq$ 2 wt. %.

Nucleation and growth are usually believed to be a process of ordering toward the thermodynamically most stable state. The Ostwald step rule is basically coherent with this view. However, we show here that the most stable state in bulk can spontaneously transform into a higher energy metastable deformed state in the growth process upon the ordering into the low-dimensional order. Although this may apparently look counterintuitive, it is quite natural considering the following characteristics of growing nuclei. The relevant energies determining the shape of nuclei are the bulk energy gain $E_{\rm bulk}$, $E_{\rm int}$, and $E_{\rm ela}$. For the smectic ordering studied here, $E_{\rm bulk} \propto R^3$, $E_{\rm int} \propto R^2$, and $E_{\rm ela} \propto R$. The last relation reflects that the lamellar phase can deform without perturbing 1D periodicity. The nucleation stage is controlled by the competition between $E_{\rm int}$ and $E_{\rm bulk}$ [Fig. 4(a)], which determines R_c. On the other hand, the growth process is controlled by the competition between $E_{\rm int}$ and $E_{\rm ela}$, which determines R_t. Once $E_{\rm int}$ exceeds $E_{\rm ela}$ (for $R \geq R_t$), the drastic shape transformation can be induced [Fig. 4(c)].

Here it may be worth noting an interesting link between this shape transformation and focal conic faceting in smectic-A liquid crystal. Fournier and Durand [15] reported that an initially planar smectic structure is transformed into focal conic domains as nuclei grow. They

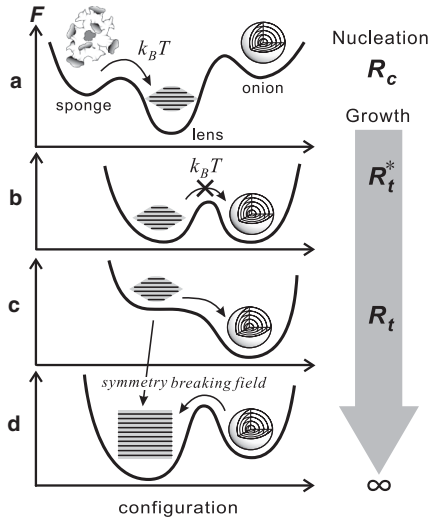

FIG. 4. Schematic free energy landscape evolution.

showed that for a large smectic-*A* domain the relative weakness of the elasticity to the interfacial energy leads to a spherical liquidlike shape. From this aspect, onion structures may be regarded as a kind of degenerate focal conics. Thus, these two phenomena share a common physical mechanism, namely, shape transformation due to a competition between elastic deformation and interfacial energy. The main difference is that for the onion structure the tangential orientation is favored at the interface, whereas for smectic-*A* liquid crystal the perpendicular orientation is favored, which leads to the texture reorganization into complex focal conic arrangements. In relation to this, a case of $\sigma_{\rm ep} < \sigma_{\rm tan}$ needs more thought. For this case, lens-shaped nuclei first transform into onion structures to reduce the interfacial energy, but then onion structures might transform into focal conics after further growth (e.g., [9]). In our case, such transformation was not observed maybe due to the large energy barrier.

Our study also provides a clear answer to a long-standing question in soft matter physics, i.e., how onion structures, which are known to be formed by shear [12], can spontaneously be formed [16–19] without shear. Our observation demonstrates that onion structures can spontaneously be formed from a lens-shaped lamellar nucleus, accompanying a quite dramatic topological change: The initial sponge phase is characterized by large negative Euler number χ_E. Then the nucleus formed first has a planar lamellar structure, whose χ_E is zero. Finally, an onion structure has a large positive χ_E. This new pathway to onion-structure formation may be primarily driven by the interfacial energy, and not by the Gaussian curvature. However, onion structures may be directly nucleated (cf. the expression of $\delta E_{\rm ela}/\delta\theta$) if $2\kappa + \kappa_g < 0$. To draw a general picture, thus, we need to clarify the respective role of the Gaussian curvature and the interfacial energy more carefully. We may at least say that the stable bulk configuration of planar lamellar order may not be formed without the help of (i) a rapid quench, for which nuclei fill up the space before shape transformation takes place, (ii) symmetry-breaking field such as surface field [8], or (iii) shear flow [20] [Fig. 4(d)]. This has a significant message concerning pattern formation in first-order phase transition: The spontaneous shape transformation of nuclei in the growth stage not only affects the kinetic pathway of ordering but also selects a metastable structure as the final structure (Fig. 4).

Finally, we note that the principle of the shape transformation may be common to any (quasi-)one-dimensional positional ordering for which $E_{\rm ela} \propto R$. However, since R_t is proportional to d [Fig. 3(a), note $\phi \propto d^{-1}$] and the characteristic time of the shape transformation also decreases steeply with decreasing d, such shape transformation in usual systems may occur much before nuclei become observable with microscopy; for example, the layer spacing is ~0.34 nm for graphite [21,22] and ~10 nm for block copolymers [23]. This may be one of the reasons the process of shape transformation has not been observed so far despite of its possible abundance. Many important materials (in nanoscience), such as block copolymers, liquid crystals, cholesterol esters, graphite, mica, and low-dimensional organic crystals, belong to this category: layered structures. For example, onion-structure formation has indeed been reported for block copolymers [23], cholesterol esters [24], and carbon (carbon onion structures [21,22]). The same physical principle may be applied for onion-structure formation in both soft and hard matter, which can be used for drag delivery [23,24] and functional devices [21,22].

The authors are grateful to C. P. Royall for critical reading of our manuscript. This work is partly supported by a grant-in-aid from the Ministry of Education, Culture, Sports, Science and Technology, Japan.

*Email address: tanaka@iis.u-tokyo.ac.jp

[1] W. F. Ostwald, Z. Phys. Chem. **22**, 289 (1897).
[2] S. Alexander and J. McTague, Phys. Rev. Lett. **41**, 702 (1978); P. R. ten Wolde and D. Frenkel, Phys. Chem. Chem. Phys. **1**, 2191 (1999).
[3] S. T. Yau and P. G. Vekilov, Nature (London) **406**, 494 (2000).
[4] M. Kleman and O. D. Lavrentovich, *Soft Matter Physics: An Introduction* (Springer, New York, 2003).
[5] Y. Iwashita and H. Tanaka, Nat. Mater. **5**, 147 (2006).
[6] S. T. Milner *et al.*, J. Phys. (France) **51**, 2629 (1990).
[7] G. Porte *et al.*, J. Phys. II (France) **1**, 1101 (1991).
[8] Y. Iwashita and H. Tanaka, Phys. Rev. Lett. **95**, 047801 (2005).
[9] C. Blanc, Phys. Rev. E **64**, 011702 (2001).
[10] C. Quilliet *et al.*, Phys. Rev. Lett. **77**, 522 (1996).
[11] O. D. Lavrentovich *et al.*, J. Phys. Chem. B **101**, 420 (1997).
[12] O. Diat and D. Roux, J. Phys. II (France) **3**, 9 (1993).
[13] Strictly speaking, this σ should be replaced by the average interfacial tension $\bar{\sigma}_{\rm lens}$, since the layer orientation is not constant for the lens-shaped structure. Note that $\sigma_{\rm tan} < \bar{\sigma}_{\rm lens} < \sigma_{\rm ep}$. Furthermore, we should use $\sigma_{\rm tan}$ instead of σ for the onion structure since the layers are exactly tangential. Here we ignore these for simplicity (see a later discussion on the validity of this approximation).
[14] C. Blanc, Soft Mater. **1**, 63 (2003).
[15] J. B. Fournier and G. Durand, J. Phys. II (France) **1**, 845 (1991).
[16] R. Gomati *et al.*, J. Phys. Chem. **91**, 6203 (1987).
[17] P. Boltenhagen *et al.*, Phys. Rev. A **46**, R1743 (1992).
[18] J. B. Fournier and G. Durand, J. Phys. II (France) **4**, 975 (1994).
[19] L. Ramos *et al.*, Europhys. Lett. **66**, 888 (2004).
[20] J. Yamamoto and H. Tanaka, Phys. Rev. Lett. **77**, 4390 (1996).
[21] D. Ugarte, Nature (London) **359**, 707 (1992).
[22] H. W. Kroto, Nature (London) **359**, 670 (1992).
[23] G. Riess, Prog. Polym. Sci. **28**, 1107 (2003).
[24] J. Kuntsche *et al.*, Pharm. Res. **21**, 1834 (2004).